A Revised Pseudo-Second-Order Kinetic Model for Adsorption, Sensitive to Changes in Adsorbate and Adsorbent Concentrations

Jay Bullen, Sarawud Saleesongsom, Kerry Gallagher, Dominik Weiss

A revised pseudo-second order kinetic model for adsorption, sensitive to changes in adsorbate and adsorbent concentrations

[1*]Jay C. Bullen; [1]Sarawud Saleesongsom; [2]Kerry Gallagher; and [1,3*]Dominik J. Weiss

[1]Department of Earth Science and Engineering, Imperial College London, London SW7 2AZ, United Kingdom

[2] Géosciences/OSUR, University of Rennes, Rennes, 35042, France

[3]Civil and Environmental Engineering, Princeton University, United States of America

*Corresponding authors:

Email: j.bullen16@imperial.ac.uk; d.weiss@imperial.ac.uk

Graphical Abstract

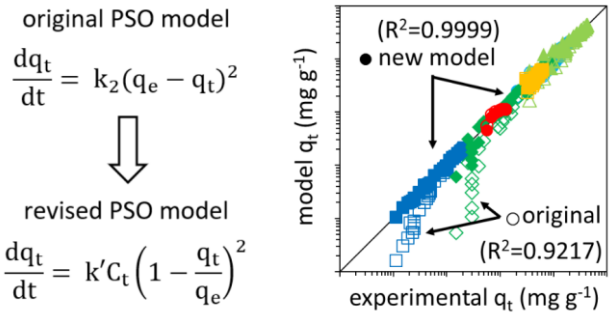

Keywords

Adsorption kinetics; kinetic model; pseudo-second order; Lagergren; water treatment; particle size

Abstract

The development of new adsorbent materials for the removal of toxic contaminants from drinking water is crucial to achieving the United Nations Sustainable Development Goal 6 (clean water and sanitation). The characterisation of these materials includes fitting models of adsorption kinetics to experimental data, most commonly the pseudo-second order (PSO) model. The PSO model, however, provides no sensitivity to changes in experimental conditions such as adsorbate and adsorbent concentrations (C_0 and C_s) and consequently is not able to predict changes in performance as a function of operating conditions. Furthermore, the experimental conditionality of the PSO rate constant, k_2, can lead to erroneous conclusions when comparing literature results. In this study, we analyse 108 kinetic experiments from 47 literature sources to develop a relatively simple modification of the PSO rate equation, yielding:

$$\frac{dq_t}{dt} = k'C_t\left(1 - \frac{q_t}{q_e}\right)^2$$

Unlike the original PSO model, this revised rate equation (rPSO) demonstrates the first-order and zero-order dependencies upon C_0 and C_s that we observe empirically. Our new model reduces the residual sum of squares by 66% when using a single rate constant to model multiple adsorption experiments with varying initial conditions. Furthermore, we highlight how the rPSO rate constant k' is more appropriate for literature comparison, highlighting faster kinetics in the adsorption of arsenic onto alumina versus iron oxides. This revised rate equation should find applications in engineering studies, especially since unlike the PSO rate constant k_2, the rPSO rate constant k' does not show a counter-intuitive inverse relationship with the increasing reaction rate when C_0 is increased.

Introduction

There is a wealth of recent literature concerning the development of novel adsorbent materials for the remediation of contaminated water, such as composite materials offering superior stability [1], ease of separation from the effluent [2 3], or multifunctional capabilities such as photocatalytic activity [4 5]. Energy input typically forms about one third of water treatment plant operation costs [6], and if energy efficiencies are to be improved then accurate models of adsorption kinetics (including rate constants) are needed to (a) identify the minimum duration needed for batch treatments and (b) estimate maximum flow rates for column or continuous-flow treatments [7]. Laboratory experiments can only partially capture the environments in which new adsorbents will operate, and in practice different concentrations of adsorbent (C_s) will be needed to treat different concentrations of contaminant in the influent (C_0). It is thus important that adsorption models are made sensitive to operating conditions, providing predictive capabilities.

The pseudo-second order (PSO) rate equation [8], popularised by Ho and McKay (1999) [9], is probably the most popular model currently used to describe adsorption kinetics [10]. The PSO rate equation takes the form:

$$\frac{dq_t}{dt} = k_2(q_e - q_t)^2$$

Equation 1

where t is time (minutes), q_t is the amount of adsorbate adsorbed per mass of adsorbent at time t (mg g^{-1}), k_2 is the pseudo-second order rate constant (g mg^{-1} min^{-1}), and q_e is the amount of adsorbate adsorbed at equilibrium (mg g^{-1}) [9].

The decrease in the concentration of aqueous adsorbate with time is given by the equation:

$$C_t = C_0 - C_S q_t$$

Equation 2

where C_t is the concentration of aqueous adsorbate at time t (mg L^{-1}), C_0 is the initial adsorbate concentration at t=0 (mg L^{-1}) and C_s is the concentration of adsorbent (g L^{-1}).

The PSO model is popular for several reasons. Firstly, it has a simple mathematical form. Secondly, despite being applied by Ho and McKay as a mechanistic model for the bidentate adsorption of copper onto peat [11], the PSO model is able to fit kinetic data for a wide range of systems with different reaction mechanisms [9 12 13] (including where diffusion control is to be expected [14]). Thirdly, Equation 1 can be integrated and rearranged to provide linear equations (of the form y=mx+c) from which the model parameters k_2 and q_e can be easily obtained by linear regression [15].

However, the PSO model has several important limitations due to the absence of adsorbate and adsorbent parameters within the rate equation, with k_2 and q_e parameters being valid only under the specific experimental conditions under which the PSO model was fitted. The first limitation is that the model cannot predict how adsorption kinetics will change as a function of C_0 and C_s, limiting its application in engineering or optimisation studies. Furthermore, rate constants from different

literature sources with different experimental conditions cannot be meaningfully compared: greater values of k_2 do not necessarily indicate adsorbents possessing superior adsorption kinetics.

The aim of the present study was to modify the popular PSO equation, introducing sensitivity towards changes in C_0 and C_s, with the objective of both improving predictive capabilities for engineering studies, and normalising rate constants for easier comparison between literature sources. The PSO model does not necessarily reveal insights into the adsorption mechanisms (i.e. whether intraparticle diffusion or chemisorption is the rate determining step) [13 16], and our aim was similarly to develop an empirical model, rather than a mechanistic model. We thus conducted an empirical analysis of the adsorption kinetics reported by the literature to assess the influence of C_0 and C_s on adsorption rates, and to modify the PSO rate equation accordingly.

We used the method of initial rates to determine the order of reaction with respect to both C_0 and C_s (given the possibility for data at later times to disguise the true reaction order [17], such as when slower surface precipitation processes coincide with monolayer adsorption [18]). We first performed quality control experiments, investigating various methods for calculating initial rates when the availability of early kinetic data is limited (as per many adsorption experiments). We then compiled a wide range of literature data sets wherein multiple adsorption kinetic experiments with different values of C_0 and C_s are reported (with each data set being a specific adsorbate-adsorbent system) and determined the order of reaction with respect to each variable. We used mineral and organic adsorbents, and metal, inorganic and organic adsorbates, to achieve a model that is generally applicable to a wide range of systems, as per the original PSO model. We built the observed C_0 and C_s dependence into a revised form of the PSO rate equation (which we refer to as *rPSO*) and verified that the rate constants given by this new model are more stable with respect to changes in experimental conditions than the PSO rate constant k_2. Finally, we used two application studies to assess the potential of this revised PSO model to overcome current limitations: (1) describing multiple experiments with varying values of C_0 and C_s using a single rate constant, and (2) achieving a more meaningful comparison of the adsorption kinetics reported across the literature.

Experimental

Data sets

Literature sources that experimentally investigated the influence of C_0, C_s or particle size upon adsorption kinetics were compiled and the experimental data tabulated (referenced in the Supplementary Information: SI Table S1). Both mineral adsorbents and organic adsorbents (activated carbon and chitosan) were included, however zeolites and metal-organic frameworks (MOFs) were not since the sorption mechanism of adsorbate trapping within cages might produce contrary results. None of the literature sources found gave any mechanistic account or mathematical explanation for observed differences in adsorption kinetics due to varying values of C_0, C_s or particle size. The majority of the compiled literature used the PSO model to describe adsorption kinetics.

In total 47 literature sources with approximately 100 kinetic experiments were collected. This includes: 14 literature sources with early kinetic data (where $0 < \frac{q_t}{q_e} < 0.2$) to investigate the influence of early data availability on calculations of the initial rate; 8 literature sources (9 data sets) with a total 37 experiments where C_0 is varied; 6 literature sources (8 data sets) with a total 27 experiments where C_s is varied; and 21 literature sources (25 experiments) for the adsorption of inorganic arsenic onto iron oxide and alumina adsorbents. A data set is considered to be all kinetic experiments using the same adsorbate-adsorbent system within a single literature source. The compiled data sets are available elsewhere [19].

Mathematical approaches for the determination of initial rates

Three approaches towards the calculation of initial rates were compared: (1) the initial slope, (2) linearised PSO kinetics, and (3) non-linear PSO kinetics.

In the initial slope approach, the initial rate ($\frac{\Delta q_t}{\Delta t}$ at t=0) was calculated as the slope between the origin at (0,0) and the earliest available data point at t>0 [20].

Initial rates were also calculated using the following linearised form of the integrated PSO rate equation:

$$\frac{t}{q_t} = \frac{1}{k_2 {q_e}^2} + \frac{t}{q_e}$$

Equation 3

Kinetic profiles were plotted as $\frac{t}{q_t}$ as a function of t and the linear regression was obtained using the LINEST function in Excel (where the residual sum of squares between the data points and the linear regression is minimised). The equilibrium adsorption parameter q_e was obtained via the relationship $q_e = \frac{1}{m}$ where m is the slope of the linear regression, and k_2 via $k_2 = \frac{1}{c \cdot {q_e}^2}$ where c is the y-intercept. The initial rate of adsorption was then calculated through the simplification of Equation 1:

$$\text{Initial rate} = \frac{dq_{t=0}}{dt} = k_2 {q_e}^2$$

Equation 4

Uncertainties in k_2, q_e and the initial rate were calculated by linear propagation of the standard errors in m and c given by the LINEST function.

Finally, initial rates were calculated using non-linear PSO kinetics. Non-linear fitting of the PSO model to experimental data was achieved by using Microsoft Excel's Solver function to optimise k_2 and q_e values, minimising the sum of squared residuals between the model and experiment. Uncertainties in k_2 and q_e were calculated using a Monte-Carlo approach with 200 simulations as described by Hu et al. [21].

For all literature sources, parameters were recalculated to the same units for ease of comparison: k_2 (g mg^{-1} min^{-1}); q_e (mg g^{-1}); and the initial rate (mg g^{-1} min^{-1}).

The influence of the availability of early kinetic data on the accuracy and precision of initial rates calculated using these three approaches was evaluated as follows. Fourteen data sets containing early kinetic data were collected (defined as adsorption experiments containing data within the range $0 < \frac{q_t}{q_e} < 0.2$). Initial rates were then re-calculated as data points were consecutively removed from the earliest to the latest. A linear regression between the calculated initial rates and the value of $\frac{q_t}{q_e}$ at the first available kinetic data was determined and extrapolated to $\frac{q_t}{q_e} = 0$ to provide a theoretical 'true' initial rate (representing if kinetic data were to be collected within an infinitesimally small time period). This theoretical 'true' initial rate was used as a reference value to determine variation in the calculated initial rate as a function of the availability of early kinetic data. A systematic error was calculated using the average error across all data sets and a random error was calculated as the standard deviation in the error across all data sets. The significance of the differences observed in the initial rate errors given by the three mathematical approaches was determined using the paired samples t-test.

After evaluating the three approaches (see Results and Discussion), non-linear PSO kinetics were used to determine initial rates in all subsequent calculations.

Determining the order of reaction

The order of reaction with respect to the independent variables C_0 and C_s was calculated as the slope of log(initial rate) versus log(independent variable) [22]. The order of reaction was calculated for each data set (kinetic experiments using the same adsorbate-adsorbent system within a single literature source), with each data point used within the linear regression representing a single kinetic experiment at a unique value of C_0 or C_s. This is represented by the equation:

$$\text{order of reaction} = \frac{\Delta \log (\text{initial rate})}{\Delta \log (C_0 \text{ or } C_s)}$$

Equation 5

For each data set, the order of reaction with respect to the independent variable was calculated using the LINEST function in Microsoft Excel. The error for each data set was specified as the standard error of the slope. An average (mean, $\bar{x}$) order of reaction representing all data sets was

calculated, with errors reported as the standard deviation. The dependencies of k_2 and k' upon C_0 and C_s were determined using the same method, only substituting the initial rate with k_2 or k'.

Modelling the revised rate equation

Our final rate equation, developed and derived in the Results and Discussion (Equation 11, referred to as the rPSO), is:

$$\frac{dq_t}{dt} = k'C_t\left(1 - \frac{q_t}{q_e}\right)^2$$

Equation 6

where the rate constant k' takes the units $L\ g^{-1}\ min^{-1}$. As the rPSO rate equation is not easily integrated, experiments were simulated using Microsoft Excel. The quantity of adsorbate adsorbed at the n^{th} data point was calculated using the following formula:

$$\mathrm{q_n} = \mathrm{q_{n-1}} + \left((\mathrm{t_n} - \mathrm{t_{n-1}}) \cdot \left(\mathrm{k'C_{t(n-1)}}\left(1 - \frac{\mathrm{q_{n-1}}}{\mathrm{q_e}}\right)^2\right)\right)$$

Equation 7

The time interval between data points, $(\mathrm{t_n} - \mathrm{t_{n-1}})$ or Δt, was reduced until the magnitude of Δt had no significant effect on the results. The rPSO parameters k' and q_e were obtained by non-linear fitting, using Microsoft Excel's Solver function to minimise the residual sum of squared residuals between the model and experiment.

For all literature sources, parameters were recalculated to the same units for ease of comparison: k_2 (g mg^{-1} min^{-1}); q_e (mg g^{-1}); and the initial rate (mg g^{-1} min^{-1}).

KERRR

$$\frac{dq_t}{dt} = k_2(q_e - q_t)^2$$

Equation 8

where t is time (minutes), q_t is the amount of adsorbate adsorbed per mass of adsorbent at time t (mg g^{-1}), k_2 is the pseudo-second order rate constant (g mg^{-1} min^{-1}), and q_e is the amount of adsorbate adsorbed at equilibrium (mg g^{-1}) [9].

The decrease in the concentration of aqueous adsorbate with time is given by the equation:

$$\mathrm{C_t} = \mathrm{C_0} - \mathrm{C_S q_t}$$

Equation 9

where C_t is the concentration of aqueous adsorbate at time t (mg L^{-1}), C_0 is the initial adsorbate concentration at t=0 (mg L^{-1}) and C_s is the concentration of adsorbent (g L^{-1}).

KERRR

201

202 ## Application studies

203 In the first application study (evaluating the potential of the rPSO model for predictive applications),
204 6 data sets were used: 3 where C_0 was varied and 3 where C_s was varied. In the first step, values of
205 the equilibrium adsorption capacity (q_e) to constrain the model were obtained by fitting kinetic
206 experiments individually using the PSO and rPSO models (optimising the rate constant and q_e
207 simultaneously to minimise the sum of squared residuals). After constraining q_e to these values, all
208 experiments within the given data set (i.e. experiments with the same adsorbate-adsorbent system
209 but different C_0 or C_s values) were simultaneously fit with the PSO and rPSO models, using a single
210 rate constant (k_2 or k', depending upon the model) to describe all experiments.

211 In the second application study (evaluating the potential of the rPSO rate constant k' for more
212 meaningful comparisons across the literature), 18 experiments reporting the adsorption kinetics of
213 inorganic arsenic onto iron oxide minerals were collated. Both As(V) and As(III) experiments were
214 included, since no significant difference between the adsorption kinetics was observed. A further 7
215 experiments reporting the adsorption of inorganic arsenic onto alumina (Al_2O_3) were collected for
216 comparison. The particle radius (r) was taken as reported by each study.

Results and Discussion

Determination of the influence of experimental conditions (C_0 and C_s) on the initial rate of adsorption

Quality control: The calculation of initial rates and setting criteria for the selection of literature data sets

Many adsorption experiments reported by the literature begin their collection of kinetic data at high values of $\frac{q_t}{q_e}$, where a significant proportion of the reaction has already been completed. This may be due to challenges in collecting samples quickly (especially when filtering is required) given that many adsorption reactions reach equilibrium in the minutes timescale. Other possible reasons include a lack of appreciation over the time-scale at which adsorption kinetics are best measured, with many papers fitting kinetic models on timescales when the reaction has already plateaued and reached equilibrium.

Whilst we chose to investigate the influence of C_0 and C_s using the method of initial rates, the lack of literature reporting early stage kinetic data (i.e. low values of $\frac{q_t}{q_e}$) is a challenge. A popular approach to calculate initial rates is to determine the slope of a line that is tangent to the experimental data curve and passes through the origin at (0,0) [20]. However, the later the first kinetic data is collected, the shallower the slope will be, creating a systematic underestimation of the initial rate. In the most extreme case, an infinite delay before collection of kinetic data will yield a slope of zero and subsequently an initial rate of zero. Application of a kinetic adsorption model allows for the extrapolation of adsorption rates to t=0, however the accuracy of the calculated initial rates depends upon how closely the experimental data obeys the applied model.

We therefore conducted a preliminary experiment to investigate how a limited availability of early kinetic data would influence the accuracy and precision of initial rates calculated using the initial slope or using the original PSO model (given that the PSO model is known to approximately describe a wide range of adsorbate-adsorbent systems [12]). These results were used to set quality control criteria for which data sets would be included within the investigation of the influence of C_0 and C_s on adsorption kinetics.

The literature search identified fourteen data sets satisfying the criteria that $\frac{q_t}{q_e} < 0.2$, a relatively small number, highlighting how most authors fail to collect early kinetic data (SI Figure S1). Initial rates calculated from the slope between the origin and the earliest available data point show the typical systematic underestimation of initial rates when early kinetic data is missing (Figure 1a, with the solid line representing the average of all data sets). In contrast, when calculated using the PSO model, there is no systematic error in the calculation of initial rates when the first kinetic data is collected in the range $0 < \frac{q_t}{q_e} < 0.7$ (Figure 1b,c). In all three approaches, significant variation between data sets is observed, i.e. an error in the initial rate unique to each data set. This error (with dashed lines representing one standard deviation) is approximately constant in the initial slope approach, being significant even when early kinetic data is available. In contrast, this error is

insignificant using early kinetic data and either of the PSO approaches, however this error increases in magnitude as early data is sequentially removed.

Additionally, the absolute values of the initial rates calculated using the earliest possible kinetic data were compared (i.e. 14 initial rate calculations), with Student's t-test indicating that both linearised PSO kinetics and non-linear PSO kinetics tend to return an initial rate greater than that calculated using the initial slope (with p=0.87 and 0.97 respectively). The increase in initial rates calculated using non-linear PSO kinetics versus linearised PSO kinetics is not significant (p=0.33 using the 14 initial rate calculations). However, when comparing the calculated initial rates with all possible data cut-offs (i.e. 115 initial rate calculations, Figure 1d) the differences are more significant: non-linear PSO kinetics return greater initial rates than linearised PSO kinetics (p=1.00). This is due to the biased weighting of linearised PSO kinetics towards data at later times, with the slope of $\frac{t}{q_e}$ versus t increasing as equilibrium adsorption is approached, returning smaller values of q_e and thus giving a smaller initial rate. The difference between initial rates calculated using linearised and non-linear PSO kinetics was observed despite equilibrium adsorption kinetic data from the original literature being excluded in our calculations.

Finally, we considered the uncertainties in the initial rates calculated using the two PSO approaches with varying availability of early kinetic data (Figure 1e). The uncertainties in the initial rates calculated using linearised PSO kinetics were calculated from the standard error in the linear regression fit to $\frac{t}{q_t}$ versus t, whilst the uncertainties in non-linear PSO kinetics were calculated using synthetic data and 200 Monte-Carlo simulations [21]. Using linearised PSO kinetics, the propagated uncertainty in the initial rate increases exponentially as early kinetic data is removed. This is explained by how late stage adsorption kinetic data is weighted too heavily when fitting linearised PSO kinetics [10], where the differences in q_t are smaller relative to the measurement uncertainty: this increases the uncertainty of the linear regression. At $\frac{q_t}{q_e} = 0.6$, the average uncertainty in the initial rates calculated using linearised PSO kinetics is 9.5%. In contrast, the uncertainty in the initial rates calculated using non-linear PSO kinetics is essentially independent of the availability of early kinetic data, and at $\frac{q_t}{q_e} = 0.6$ the average uncertainty is only 5.7%.

As highlighted here, ideally the data sets used to explore the influence of experimental parameters such as the adsorbate concentration (C_0) and the adsorbent concentration (C_s) should include early kinetic data to reduce the uncertainty in the calculated initial rates. However, literature data reporting early adsorption kinetics is limited. To provide a balance between the accuracy of our initial rate calculations and the collection of a sufficient quantity of data sets for statistical analysis, we set the criterion that data sets must include kinetic data with $\frac{q_t}{q_e} < 0.6$. This boundary condition gives an average error in the calculated initial rate of -44 ±22 % for the initial slope approach, +17 ±38 % using linearised PSO kinetics, and only +3 ±27% for the non-linear PSO kinetics. The results indicate that non-linear PSO kinetics are most appropriate for calculating initial rates, with an insignificant systematic error. A ~30% uncertainty remains, associated with how closely the adsorption kinetics fit to the PSO form (with deviations being both due to inaccurate measurements and real chemical mechanisms).

By considering a literature source reporting two kinetic experiments only, with a different value of C_0 or C_s in each, a 30% error in the initial rate of the first experiment (as per the boundary condition of $\frac{q_t}{q_e} < 0.6$) will confer an error of <0.5 in the calculated reaction order. In this work, the average value of $\frac{q_t}{q_e}$ in the first available kinetic data was 0.37 for experiments where C_0 is varied, and 0.27 for experiments were C_s is varied. Furthermore, the number of kinetic experiments in each literature data set was 3-6, indicating that the uncertainties in the calculated initial rates will be <30%. Under these conditions, the calculated orders of reaction will be accurate to the nearest integer value. This was deemed appropriate for the purposes of developing the revised PSO model, given that it is common practice for kinetic adsorption models to use integer values for reaction orders (e.g. the original PSO equation, and the pseudo-first order kinetic model [9]). In principle, however a similar analysis could be made relaxing this condition.

Consequently, non-linear fitting of the PSO model was used to determine the initial rate of adsorption in each kinetic experiment in all subsequent work.

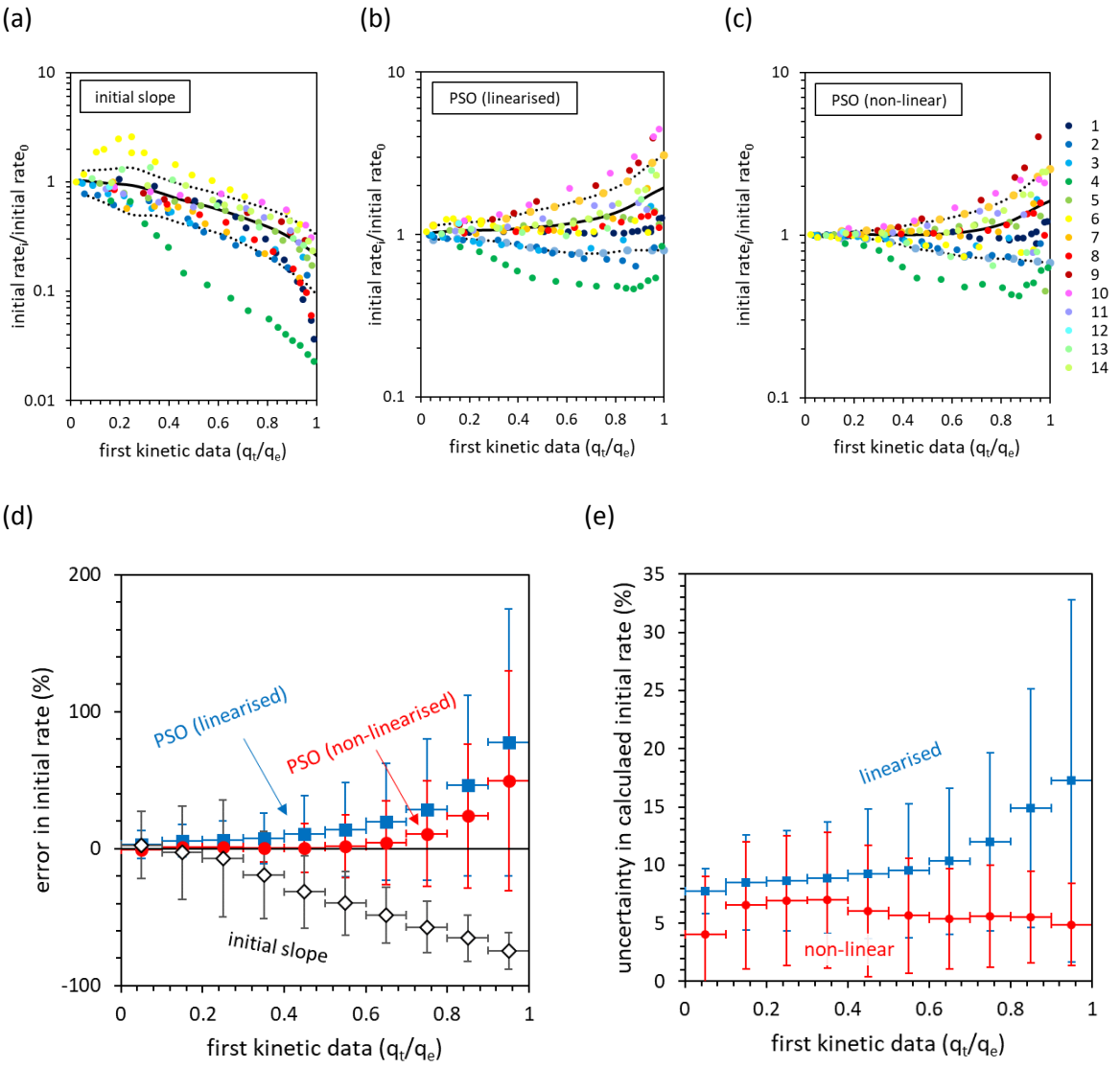

Figure 1: The influence of the limited availability of early kinetic data on the calculation of initial rates of adsorption, assessed by the analysis of 14 literature sources. The influence of removing early kinetic data on the calculated initial rates was assessed using (a) the initial slope, (b) linearised PSO kinetics, and (c) non-linear PSO kinetics. The theoretical 'true' initial rate is given by initial $rate_0$ *and the initial rate calculated with the available data given by* initial $rate_i$. *The solid black line represents the average of the 14 data sets, whilst dotted lines indicate one standard deviation. The three approaches are compared, assessing the influence of data availability on (d) the relative error in the initial rate, and (e) the uncertainty in the calculated initial rate. The horizontal error bars in (d) and (e) represent the size of the bins used for grouping data, whilst the vertical error bars indicate the standard deviation calculated between the 14 unique data sets. The data sets listed are in order: (1) Yang et al., 2019 [23], (2) Yang et al., 2001 [24], (3 and 4) Liu and Shen, 2008 [25], (5) Zhu et al. 2016 [26], (6) Yang et al. 2019 [27], (7) Yang et al. 2019 [28], (8) Mohamed et al. 2007 [29], (9) Drenkova-tuhtan et al. 2015 [30], (10) Liu et al. 2016 [31], (11) Ornek et al. 2007 [32], (12) Zhan et al. 2018 [33], (13) Ai et al. 2020 [34], (14) Nadiye-tabbiruka and Sejie 2019 [35].*

Determining the influence of C_0 and C_s upon the rate of adsorption and the PSO rate constant k_2

The influence of C_0 and C_s upon the initial rate of adsorption (calculated as the rate at t=0 using non-linear PSO kinetics) is presented in Figure *2*. For each data set, the order of reaction was determined from the slope of log(initial rate) versus log(C_0) or log(C_s) (Figure *2*a,b). Based upon the evaluation of uncertainties in the initial rates calculated using non-linear PSO kinetics (in the previous section), the reaction orders are accurate to the nearest integer value. The data sets tend to show a first-order dependency of initial rate upon the initial adsorbate concentration (C_0) (Figure *2*c), with an average dependency and standard deviation of 0.80 ±0.38, and a median value of 0.67. Of the 9 data sets, 7 were closest to first-order dependency, and 2 were closer to zero-order dependency. The sum of normal distributions representing the reaction orders and uncertainties calculated for each data set was approximated by a single normal distribution. (However, a larger number of data sets are needed to verify this). Based upon the standard deviation and assuming a normal distribution in the results, the relationship between the initial rate and C_0 is first-order with a 90% confidence interval (1.65 standard deviations). This is intuitive for both diffusion and adsorption-controlled mechanisms, as twice as much adsorbate should lead to twice as much adsorbate flux from adsorbent surface into pores, and collisions with the adsorbent surface should be twice as frequent [36 9].

A first-order dependency of initial rates (normalised to *mg* L^{-1} *min*$^{-1}$) with respect to the adsorbent concentration (C_s) is also observed (Figure *2*d), albeit with a wider distribution of results: an average value of 1.11 ±0.33 and a median of 1.07. Of the 8 data sets, 6 were closest to first-order dependency, with 1 data set closer to zero-order and another closer to second-order. Based upon the standard deviation and assuming a normal distribution in the results, the relationship between the initial rate and C_s is also first-order with a 90% confidence interval (1.65 standard deviations). This is again intuitive for both diffusion and adsorption-controlled mechanisms, as when C_s is doubled the total surface area available to solution (m^2 L^{-1}) is doubled, the overall flux of adsorbate entering adsorbent pores is doubled, and the rate of collisions between adsorbate and total adsorbent surface is also doubled. When normalised to mass (mg g^{-1} min^{-1}) the initial rate is zero-order with respect to C_s, as expected.

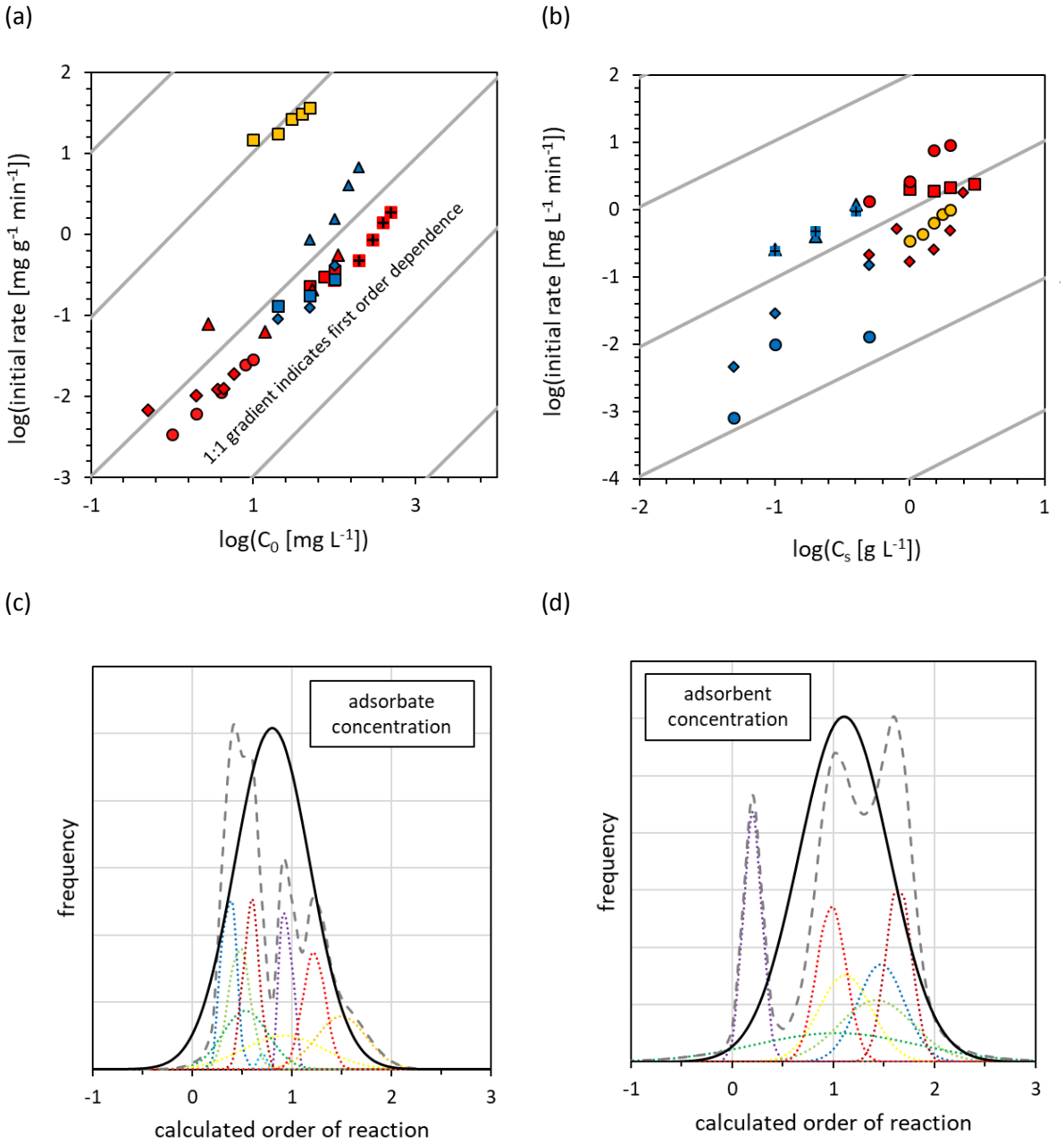

Figure 2: Determining the influence of initial adsorbate concentration (C_0) and adsorbent concentration (C_s) on the initial rate of adsorption using literature data sets. The order of reaction was determined from the slope of log(initial rate) as a function of (a) log(C_0) and (b) log(C_s), with each data point representing a single kinetic experiment (with unique values of C_0 and C_s). All experiments in a given data set (one literature paper, where all experimental conditions except for either C_0 or C_s are constant) are grouped by colour and symbol, with oxyanions in red, metal cations in blue, and organic dyes in yellow (a legend referencing the literature sources is presented in SI Figure S2). Uncertainties were calculated from the standard error in the slope. The results are alternatively presented using normal distributions with the mean given by the slope and the standard deviation given by the standard error of the slope (c and d). Here, each data set is represented by a dotted line, and the sum of all data sets given by the dashed line. Solid black lines represent the normal distribution obtained by the average of all data sets.

For both predictive modelling and the comparison of adsorption kinetics between literature sources, it is necessary that rate constants are not affected by the experimental conditions. Whilst adsorption kinetics are typically first-order with respect to C_0, the PSO rate constant k_2 is inversely proportional

to C_0 (Figure 3a). Consequently, whilst doubling the initial adsorbate concentration typically increases the initial rate of adsorption by a factor of two, counter-intuitively the PSO rate constant k_2 will decrease by a factor of two. The average slope of $\log(k_2)$ versus $\log(C_0)$ is -0.73±0.46. The inverse relationship between k_2 and C_0 is explained by the second-order dependence of the PSO model upon the **absolute** concentration of available adsorption capacity remaining through the term $(q_e-q_t)^2$. In cases where the adsorbent is unsaturated, increasing C_0 by a factor of two will approximately double q_e. The parameter $(q_e-q_t)^2$ at t=0 will increase by a factor of four, and consequently k_2 must decrease by a factor of two to achieve the observed doubling of initial rates.

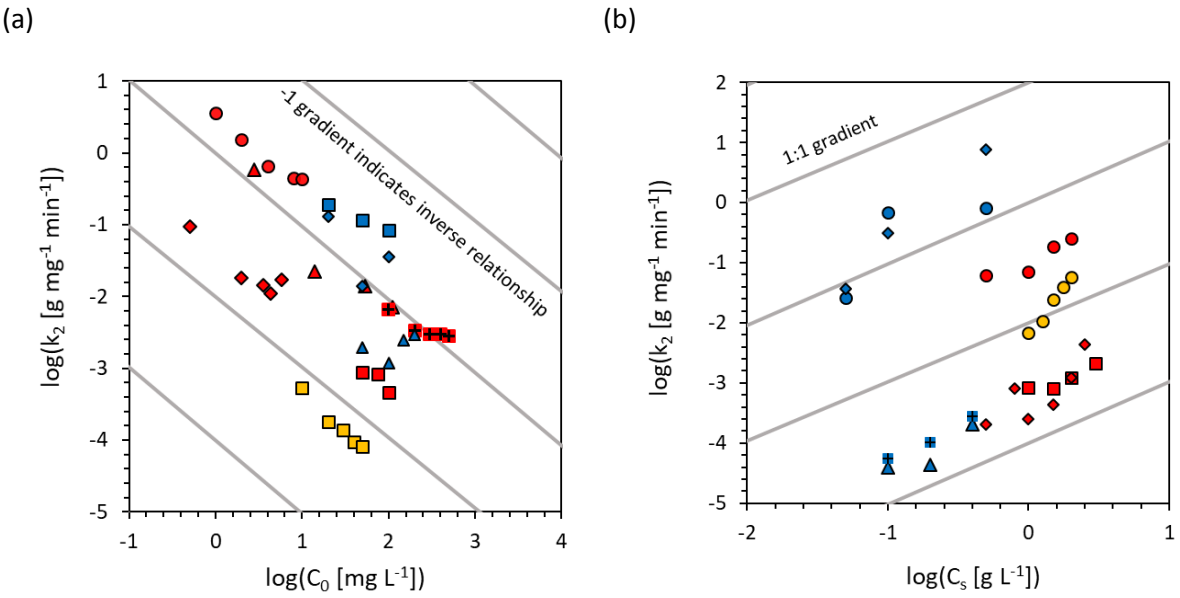

Figure 3: Dependence of the pseudo-second order (PSO) rate constant k_2 upon (a) initial adsorbate concentration (C_0), and (b) adsorbent concentration (C_s). The data is presented as described in Figure 2, with a legend referencing the literature sources presented in SI Figure S2.

In contrast, a positive relationship between C_s and k_2 is observed, with an average dependency of 1.57±0.85 (Figure 3b). (First and second-order dependencies between k_2 and C_s are both included within the standard deviation). This is explained by how when C_s is doubled, q_e will decrease by a factor of between 0 and 2: zero when the adsorbate is in excess and q_e is insignificant compared to C_0, and two when the adsorbent is in excess and q_e is large relative to C_0. Consequently, as C_s increases, $(q_e-q_t)^2$ decreases with a zero-to-second-order dependency, and to achieve the zero-order relationship between C_0 and initial rates (mg g^{-1} min^{-1}), k_2 must also increase with a dependency that is between zero and second-order.

Revision of the pseudo-second order (PSO) rate equation to account for changes in adsorbate (C_0) and adsorbent (C_s) concentrations

Modification of the PSO rate equation

In this section, we modify the original PSO rate equation to include the appropriate sensitivity towards C_0 and C_s, meeting the aims of (a) improving the predictive capacity of this model, and (b) normalising rate constants for better comparison across the literature.

Firstly, for a given concentration of adsorbent, the total concentration of adsorption surface sites is constant regardless of the value of C_0. The term within the rate equation used to represent the contribution of adsorption surface site availability towards the rate of reaction should therefore be independent of C_0. The original PSO rate equation contains a second-order dependence upon the **absolute amount** of adsorption capacity remaining, $(q_e\text{-}q_t)^2$, which gives the undesirable inverse relationship between the rate constant and C_0 demonstrated in Figure 3a. This term can be replaced with a second-order dependence upon the **relative amount** of adsorption capacity remaining, $\left(1-\frac{q_t}{q_e}\right)^2$, which will always return a value of 1 at time t=0, independent of C_0. This term therefore describes the contribution of adsorption surface site availability towards the rate of adsorption more appropriately than the original PSO term $(q_e\text{-}q_t)^2$. Here, $\frac{q_t}{q_e}$ is the same as the parameter θ used in the Langmuir adsorption isotherm model [20]. This modification of Equation 1 gives the following:

$$\frac{dq_t}{dt} = k''\left(1-\frac{q_t}{q_e}\right)^2$$

Equation 10

where $k'' = k_2 {q_e}^2$.

The first-order dependence of the reaction rate upon the adsorbate concentration observed experimentally (Figure *2*c) is then defined within the rate equation, giving:

$$\frac{dq_t}{dt} = k' C_t\left(1-\frac{q_t}{q_e}\right)^2$$

Equation 11

where $k' = \frac{k_2 {q_e}^2}{C_0}$. The rate constant k' takes the units *L* g^{-1} min^{-1}.

The initial rate of adsorption tends to be zero-order with respect to C_s (when normalised to adsorbent mass with the units *mg* g^{-1} min^{-1}). The original PSO model gives an initial rate that varies with changes in C_s, due to its second-order dependence upon the absolute adsorption capacity remaining $(q_e\text{-}q_t)^2$ and the decrease in q_e with increasing C_s. In contrast, since the rPSO depends on the relative adsorption capacity remaining through the term $\left(1-\frac{q_t}{q_e}\right)^2$, this rate equation displays the zero-order dependency of C_s identified from analysis of the literature. The rPSO rate constant k' is therefore theoretically independent of changes in C_s, unlike the original PSO rate constant k_2. The

rPSO model is similar to the adsorption-only form of the kinetic Langmuir model (kLm), which at high surface coverage is first order with respect to C_t and second order to $(1 - \frac{q_t}{q_e})$ [37] [38].

Validation of the rPSO rate equation

The removal of experimental conditionality (i.e. the dependency upon C_0 and C_s) from the revised model was verified using experimental data from the literature. The ideal rate constant is unaffected by the experimental conditions, and subsequently the dependency of the rate constant with respect to C_0 and C_s should be zero. These dependencies were calculated from the slope of log(rate constant) versus log(C_0) or log(C_s). As highlighted by Figure 4a, the original PSO rate constant k_2 is strongly dependent upon the experimental conditions, being inversely proportional to C_0 and second-order with respect to C_s. The average C_0 dependency is -0.73±0.46, and the average C_s dependency is 1.57±0.79. In contrast, k' is approximately zero-order with respect to both experimental variables. Furthermore, the dependencies of k' upon C_0 and C_s vary less (there is less scattering) than k_2. The average C_0 dependency is -0.20±0.38 and the average C_s dependency is 0.10±0.45. These results demonstrate that the new rate constant k' is less conditional than k_2, and that the dependency of adsorption kinetics upon C_0 and C_s is captured by the new model.

When the adsorbate is in excess (q_e<C_0) the rPSO model approximates the form of the original PSO model. At higher values of q_e relative to C_0, the graphical form of the two models deviates, due to the rPSO kinetics decreasing more rapidly than PSO kinetics due to the consumption of the adsorption, which decreases the parameter C_t. (However, this effect is logical, given that at low C_t values, the rate of adsorption will be limited by the availability of adsorbate). Therefore, rate constants for the rPSO (k') can be readily calculated from PSO parameters k_2 and q_e when the adsorbate is in excess, using the formula $k' = \frac{k_2 {q_e}^2}{C_0}$. When the adsorbent removes the majority of the adsorbate, however, the rPSO model will require re-fitting due to the increasing difference in the graphical form of the PSO and rPSO models.

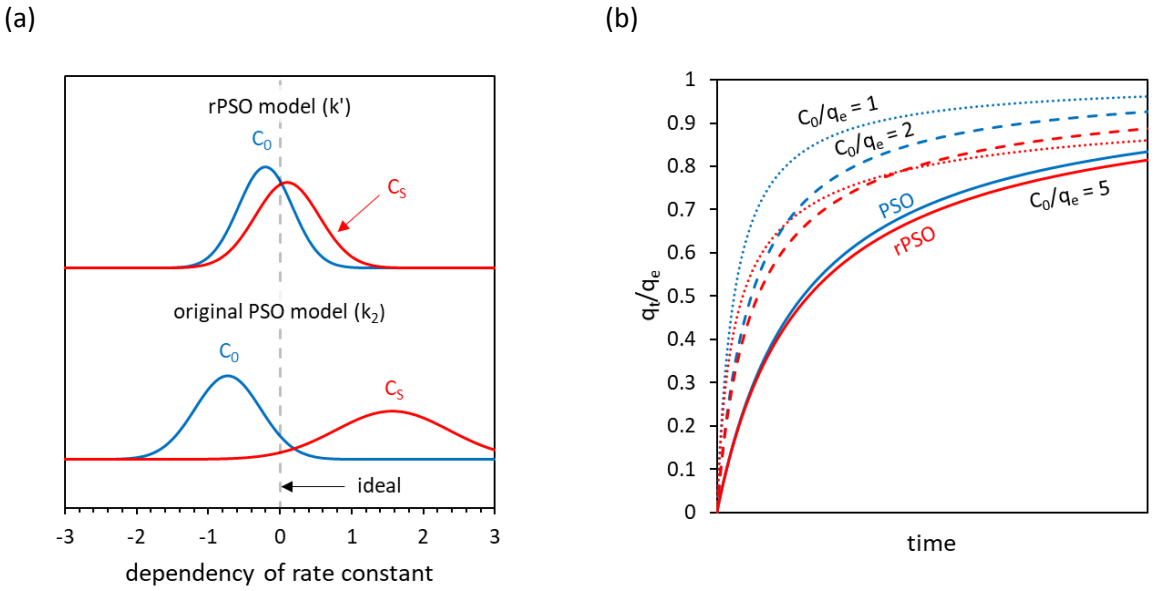

Figure 4: Verifying that experimental conditionality (with respect to C_0 and C_s) is decreased in the rPSO model versus the original PSO model. (a) The dependencies of the original PSO rate constant k_2 and the rPSO rate constant k' upon C_0 and C_s were calculated from the slope of log plots, as per Figure 3, with the ideal rate constant giving a reaction order or 'dependency' of zero. The data is shown as normal distributions with the mean and standard deviation set equal to the slope and standard error of the slope in the log plots (with 9 data sets for C_0 and 8 for C_s). These values are: -0.73±0.46 for k_2 and C_0; 1.57±0.79 for k_2 and C_s; -0.20±0.38 for k' and C_0; 0.10±0.45 for k' and C_s. (b) A comparison of the form of the original PSO equation with the rPSO equation, with different $\frac{C_0}{q_e}$ ratios (with C_s=1 g L^{-1}). The original PSO model is presented in blue and the rPSO model in red, with $\frac{C_0}{q_e}$ equal to 1 (dotted lines), 2 (dashed lines), and 5 (solid lines).

Example applications

Application 1: Evaluating the predictive capability of the revised PSO model

The first objective of this work was to provide a simple modification of the popular PSO model to introduce predictive capabilities, for the purpose of engineering studies [39]. If the kinetic model is to be used to predict adsorption performance under different conditions, then it is essential that the model parameters obtained experimentally are valid in a range of scenarios. Consequently, we evaluated whether the rPSO model would provide a better fit to experimental data compared against the PSO model, if a single rate constant is used to model multiple experiments with different values of C_0 and C_s.

The original PSO model tends to systematically overestimate q_t for experiments with high C_0 or low C_s values and systematically underestimate q_t for experiments with low C_0 or high C_s values (Figure 5). This is due to the negative and positive relationships between k_2 and C_0 and C_s respectively as previously discussed, with this relationship being denied when a single value of k_2 is used to model all experiments. The rPSO model gave a better fit to experimental data (i.e. a smaller sum of squared residuals) in 5 of the 6 data sets tested (all panels in Figure 5 except d) and the median decrease in the sum of squared residuals when changing from the PSO to the rPSO model was 66%.

(a)

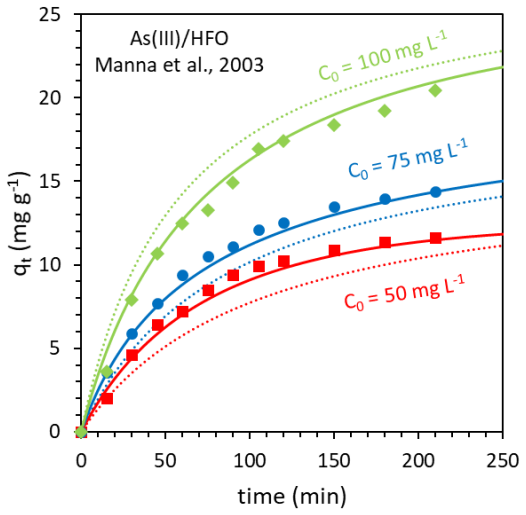
As(III)/HFO
Manna et al., 2003
C_0 = 100 mg L^{-1}
C_0 = 75 mg L^{-1}
C_0 = 50 mg L^{-1}
q_t (mg g^{-1})
time (min)

(b)

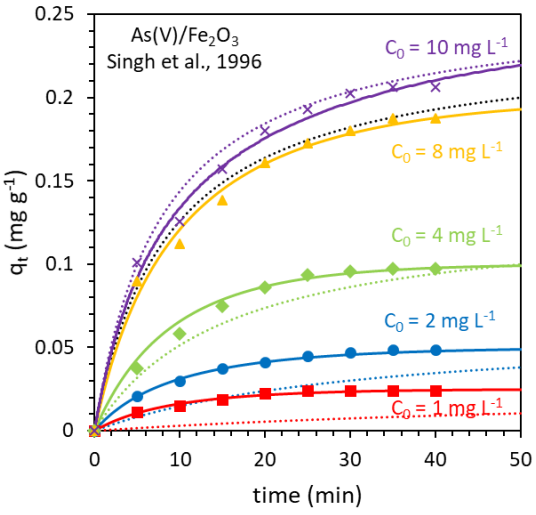
As(V)/Fe_2O_3
Singh et al., 1996
C_0 = 10 mg L^{-1}
C_0 = 8 mg L^{-1}
C_0 = 4 mg L^{-1}
C_0 = 2 mg L^{-1}
C_0 = 1 mg L^{-1}
q_t (mg g^{-1})
time (min)

(c)

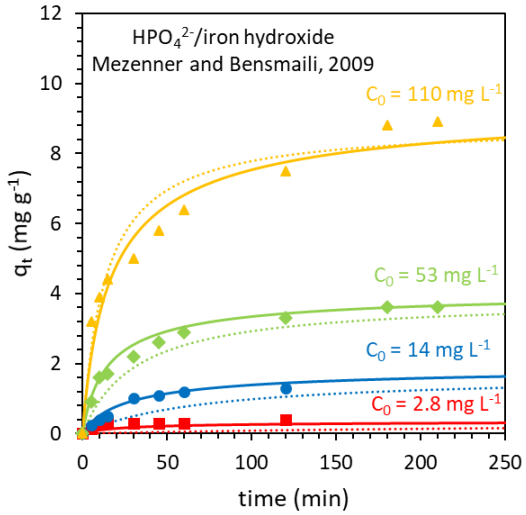
HPO_4^{2-}/iron hydroxide
Mezenner and Bensmaili, 2009
C_0 = 110 mg L^{-1}
C_0 = 53 mg L^{-1}
C_0 = 14 mg L^{-1}
C_0 = 2.8 mg L^{-1}
q_t (mg g^{-1})
time (min)

(d)

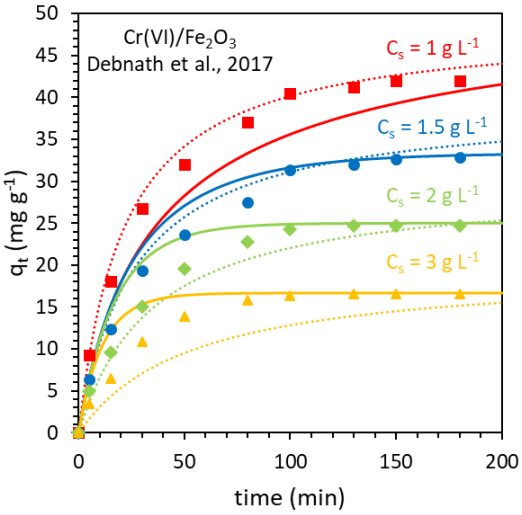
Cr(VI)/Fe_2O_3
Debnath et al., 2017
C_s = 1 g L^{-1}
C_s = 1.5 g L^{-1}
C_s = 2 g L^{-1}
C_s = 3 g L^{-1}
q_t (mg g^{-1})
time (min)

(e)

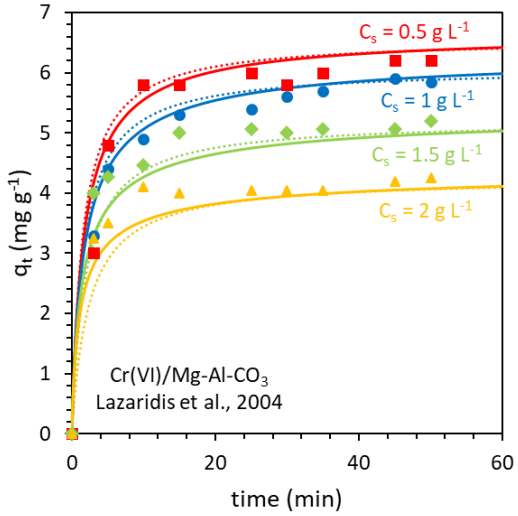
C_s = 0.5 g L^{-1}
C_s = 1 g L^{-1}
C_s = 1.5 g L^{-1}
C_s = 2 g L^{-1}
Cr(VI)/Mg-Al-CO_3
Lazaridis et al., 2004
q_t (mg g^{-1})
time (min)

(f)

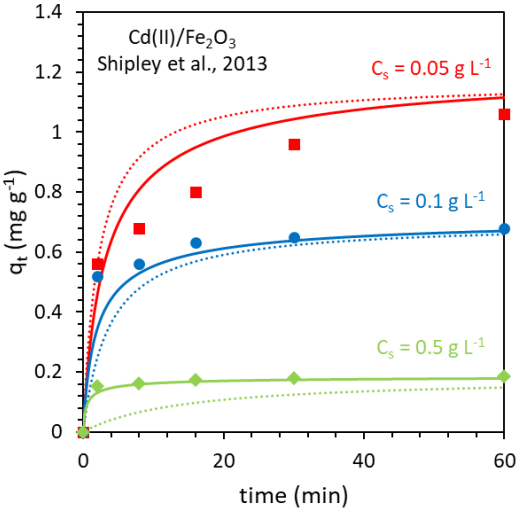
Cd(II)/Fe_2O_3
Shipley et al., 2013
C_s = 0.05 g L^{-1}
C_s = 0.1 g L^{-1}
C_s = 0.5 g L^{-1}
q_t (mg g^{-1})
time (min)

Figure 5: Application study 1: Application of the revised PSO (rPSO) model (solid lines) to describe multiple experiments with a single rate constant, compared against the original PSO model (dotted lines). (a,b,c) present 3 experiments where C_0 is varied, and (d,e,f) present 3 experiments where C_s is varied. Experimental data was sourced from Manna et al. (2003) [40], Singh et al. (1996) [41], Mezenner and Bensmaili (2009) [42], Debnath et al. (2017) [43], Lazaridis et al. (2004) [44], and Shipley et al. (2013) [45].

The average relative error of q_t calculated by the rPSO is just 1±17%, versus -11±27% for the original PSO model (Figure 6a), indicating that the rPSO model provides greater accuracy when modelling adsorption kinetics with changing values of C_0 and C_s using a single rate constant. Furthermore, the calibration curve of q_t (model) against q_t (experiment) is closer to the ideal one-to-one line in the rPSO model, with an R^2 value of 0.999 versus just 0.9217 for the original PSO model (Figure 6b). Considering each experimental data series in turn, the typical slope of the calibration curve was closer to one, with less scattering, in the rPSO model (a slope of 0.99±0.11) compared against the original PSO model (with a slope of 1.23±0.35) (Figure 6c).

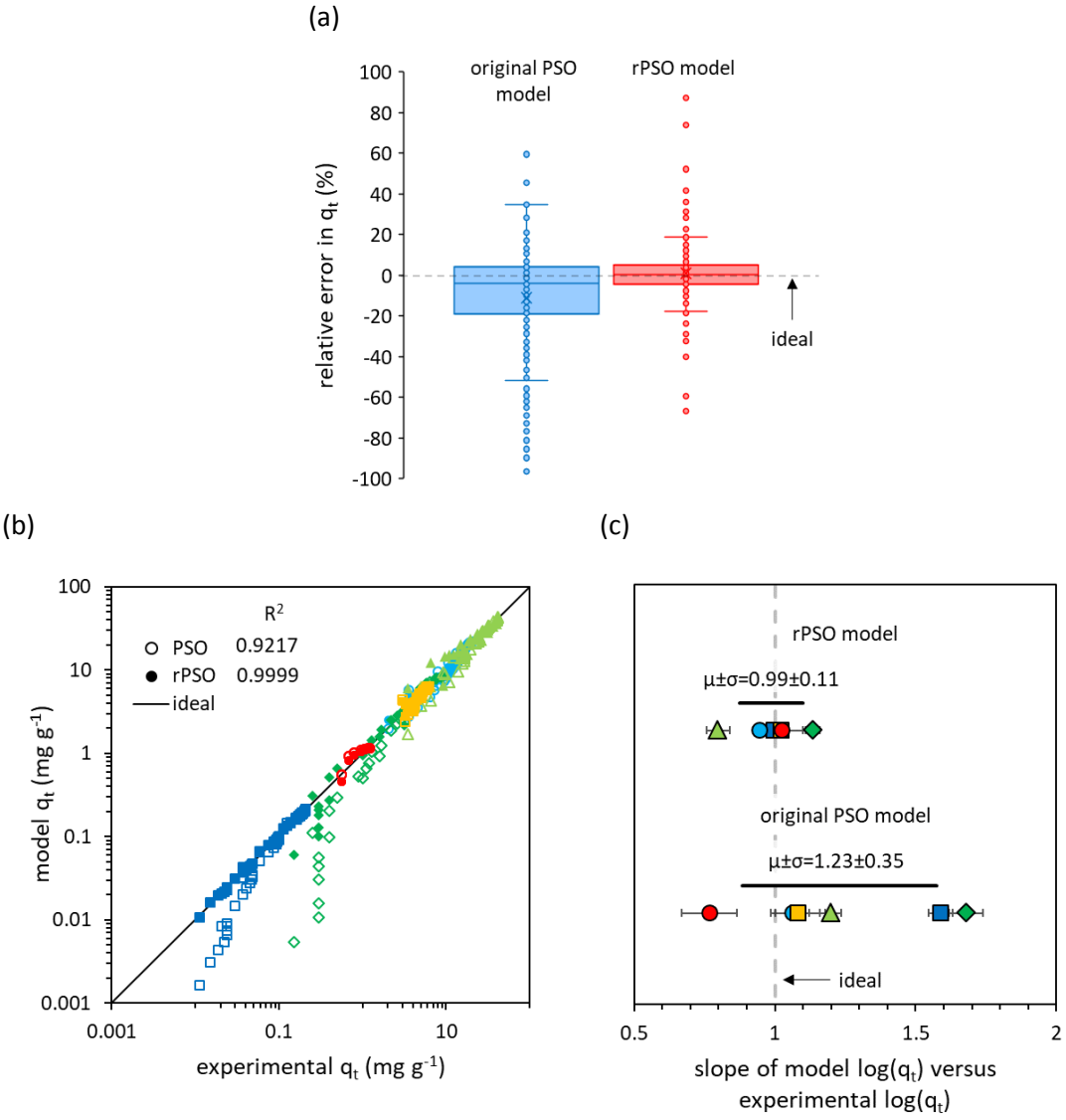

Figure 6: Application study 1: Cross-calibration of the rPSO model against experimental data (6 literature sources, 22 experiments and 198 data points). (a) Box and whisker plot presenting the relative error of q_t calculated via the original PSO model and the rPSO model. The boxes highlight the 25%, 50% (median) and 75% percentiles, whilst the whiskers represent

the minima and maxima excluding 'outlier' data points, defined as those greater than the top of the box plus 1.5 times the interquartile range, or less than the bottom of the box minus 1.5 times the interquartile range. (b) Cross-calibration plot highlighting the goodness of fit against the one-to-one line. Open shapes indicate q_t values calculated using the original PSO model, whilst filled shapes indicate the rPSO model. Values of R^2 indicate the goodness of fit against the ideal one-to-one line. (c) Comparison of the cross-calibration slopes with each model and each data set. Literature sources are denoted as As(III)/HFO [40] (dark blue squares), As(V)/Fe_2O_3 [41] (light blue circles), HPO_4^{2-}/iron hydroxide [42] (dark green diamonds), Cr(VI)/Fe_2O_3 [43] (light green triangles), Cr(VI)/Mg-Al-CO_3 [44] (orange squares), and Cd(II)/Fe_2O_3 [45] (red circles). Further results are presented in SI Figure S3.

Whilst the rPSO rate constant k' appears to be more stable to changes in experimental conditions than the PSO rate constant k_2, the parameter q_e is conditional, depending upon C_0 and C_s. For predictive modelling, this limitation can be rectified by using an adsorption isotherm to predict q_e (such as the Langmuir or Freundlich model [46]). Though a single value of q_e can be determined for the entirety of each experiment, in scenarios such as a column reactor the equilibrium adsorbate concentration parameter C_e has diminished physical significance, and it may be better to replace this term with C_t, recalculating the hypothetical value of q_e at each point in time. Huang et al. previously demonstrated that this approach can give a better account of the true driving force of the reaction during the initial stages of adsorption [47].

Application 2: Comparison of rate constants between different experimental studies

Comparison of the rPSO rate constant k' is expected to be more meaningful and more appropriate than k_2 when comparing the adsorption kinetics reported in the literature using different experimental conditions, since some of the experimental conditionality (towards changes in C_0 and C_s) is accounted for. To demonstrate the potential application of normalised rate constants towards achieving a meaningful comparison of the adsorption kinetics reported across the literature, we collected 14 and 7 literature sources reporting the kinetics of inorganic arsenic As(V) and As(III) adsorption onto iron oxide and alumina adsorbents respectively.

The average value of $\log(k_2)$ for all iron oxide studies is -0.93±1.50, whilst the average of log(k') is -1.05±1.08. In both cases, the standard deviation is large, with more than an order of magnitude variation in k_2 and k' values: neither model provides a rate constant that is generally valid for iron oxide adsorbents used by different studies. Similarly, the adsorption of inorganic arsenic onto alumina gives average values of $\log(k_2) = 0.98\pm1.84$ and $\log(k') = 0.35\pm1.75$.

Whilst the variation in both k_2 and k' across the literature is large, the influence of adsorbent morphology on adsorption kinetics has not been incorporated into either of the PSO and rPSO models. Adsorption kinetics are often faster for adsorbent materials with smaller particles, due to the improved rate of mass transport of the adsorbate to adsorbent surface sites [48]. For instance, in intraparticle diffusion model gives a rate of adsorption that is proportional to r^{-1} (where r is particle size) [49].

Whilst a faster reaction is anticipated for small iron oxide particle sizes, plotting $\log(k_2)$ as a function of $\log(r^{-1})$ shows a weak inverse relationship (linear regression gives a slope of -0.49±0.20 and R^2=0.3234) (Figure 7a). This is due to the significant increase in q_e as the particle size decreases (SI Figure S4) and the inverse relationship between k_2 and q_e through the term $(q_e-q_t)^2$ as previously

discussed. In contrast, alumina shows the anticipated positive relationship (with a slope of 0.61±0.28 and R^2=0.4783). Since adsorption onto smaller particles is typically faster than onto larger particles, the comparison of k_2 values for different adsorbent sizes and different adsorbent materials (i.e. iron oxides versus alumina) is not useful and is likely to lead to false conclusions.

In contrast, we see the anticipated positive relationship for log(k') as a function of log(r^{-1}) for both iron oxide and alumina adsorbents (Figure 7b). For the iron oxides we see a slope of 0.44±0.1 with R^2=0.5211, and for alumina we see a slope of 0.62±0.25 and R^2=0.5547. The limited goodness of fit in the linear regression is controlled by factors including poor characterisation of the particle size and differences in experimental conditions beyond C_0 and C_s, such as the pH. The accurate characterisation of particle size is especially challenging, given the range of techniques used by the literature including transmission electron microscopy (TEM), dynamic light scattering (DLS) and sieve fractionation.

The results from this literature survey show greater values of log(k') at each specific particle size for alumina versus iron oxides, suggesting that the adsorption of inorganic arsenic is faster onto alumina than onto iron oxides. With more rigorous analysis, such a study would have important implications in the design of engineered solutions for arsenic remediation, i.e. opting to use alumina in place of iron oxides when high flow rates in a column filter are required, or when larger particle sizes are necessary to achieve the desired flow rate and porosity. This highlights that normalisation of the PSO rate constant k_2 to the rPSO rate constant k', or some other constant, can achieve a more meaningful comparison of the adsorption kinetics reported by the literature.

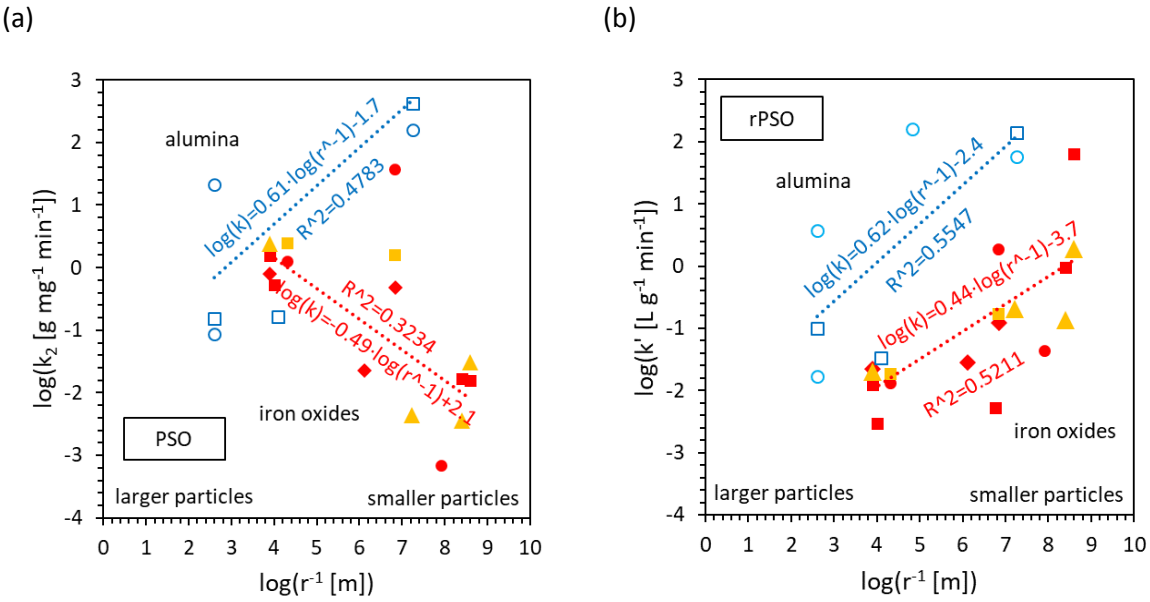

Figure 7: Application study 2: Use of the rPSO rate constant k' to compare literature sources with adsorption kinetics determined under different experimental conditions. Particle size decreases from left to right. Presented are As(V) (red filled shapes) and As(III) (orange filled shapes) adsorption onto iron oxides, and As(V) (dark blue open squares) and As(III) (light blue open circles) adsorption onto alumina. Each data point indicates a different literature source, with a legend given in SI Figure S5.

Conclusions

This work aimed to modify the popular pseudo-second order (PSO) model of adsorption kinetics to remove experimental conditionality, focusing upon initial adsorbate concentration (C_0) and adsorbent concentration (C_s). A revised PSO rate equation (rPSO) was developed from the empirical analysis of 69 kinetic experiments taken from 15 literature sources. The final equation takes the form $\frac{dq_t}{dt} = k'C_t(1-\frac{q_t}{q_e})^2$. The first application study demonstrates that the rPSO equation allows for a single rate constant to model multiple experiments, differing in the experimental conditions C_0 and C_s, with greater accuracy and a 66% decrease in the sum of squared residuals versus the original PSO model. The second application study demonstrates that the rPSO equation provides a rate constant which is more useful for comparison across the literature than the PSO rate constant k_2, obeying the anticipated relationship between adsorption rates and particle size.

The new rate equation is similar to an adsorption-only form of the kinetic Langmuir model (kLm), which at high surface coverage is first order with respect to C_t and second order with respect to $(1-\frac{q_t}{q_e})$ [37] [38]. However, the rPSO equation is simpler, with fewer fitting parameters needed, and may thus be more useful for the non-expert. The rPSO equation may prove more useful than the original PSO model in engineering studies where operating conditions are likely to vary.

One of the reasons for the popularity of the original PSO model is its linearised forms, from which k_2 and q_e parameters can be readily obtained from experimental data. Whilst, we have unfortunately not yet found a way to linearise the rPSO rate equation, it is worth noting that linearisation of the original PSO model often results in a poorer quality of fit versus when using non-linear fitting [14]. Where necessary, the rate constant for this revised model can be quickly obtained from linearised PSO kinetics using the expression $k' = \frac{k_2 {q_e}^{\dagger 2}}{{C_0}^{\dagger}}$.

In our analytical approach, we demonstrate that non-linear fitting of PSO kinetics is more appropriate than linearised PSO kinetics and the initial slope approach when early kinetic data is limited, as is often the case in adsorption experiments. Our literature survey only yielded 9 data sets where C_0 was varied and 8 where C_s was varied, satisfying our requirements for early kinetic data with $\frac{q_t}{q_e} < 0.6$. This highlights a need for experimental work to investigate the influence of these independent variables more systematically, and to ensure that initial adsorption kinetics are adequately captured, given that the method of initial rates is typically considered the superior approach towards determining reaction orders [17].

Acknowledgements

The authors acknowledge support from the Engineering Physical Sciences Research Council (EPSRC) [grant number EP/N509486/1].

Supporting information

The supplementary information provides references to all data sets used in this work; figures showing the influence of adsorbent morphology on k_2; and tabulates all parameters (q_e, k_2, k' and initial rate) calculated in this work.

References

(1) Boddu, V. M.; Abburi, K.; Randolph, A. J.; Smith, E. D. Removal of Copper(II) and Nickel(II) Ions from Aqueous Solutions by a Composite Chitosan Biosorbent. *Sep. Sci. Technol.* **2008**, *43* (6), 1365–1381. https://doi.org/10.1080/01496390801940762.

(2) Linghu, W.; Yang, H.; Sun, Y.; Sheng, G.; Huang, Y. One-Pot Synthesis of LDH/GO Composites as Highly Effective Adsorbents for Decontamination of U(VI). *ACS Sustain. Chem. Eng.* **2017**, *5* (6), 5608–5616. https://doi.org/10.1021/acssuschemeng.7b01303.

(3) Deng, L.; Shi, Z.; Peng, X. Adsorption of Cr(VI) onto a Magnetic CoFe2O4/MgAl-LDH Composite and Mechanism Study. *RSC Adv.* **2015**, *5* (61), 49791–49801. https://doi.org/10.1039/c5ra06178d.

(4) D'Arcy, M.; Weiss, D.; Bluck, M.; Vilar, R. Adsorption Kinetics, Capacity and Mechanism of Arsenate and Phosphate on a Bifunctional TiO2-Fe2O3 Bi-Composite. *J. Colloid Interface Sci.* **2011**, *364* (1), 205–212. https://doi.org/10.1016/j.jcis.2011.08.023.

(5) Chi, S.; Ji, C.; Sun, S.; Jiang, H.; Qu, R.; Sun, C. Magnetically Separated Meso-g-C3N4/Fe3O4: Bifuctional Composites for Removal of Arsenite by Simultaneous Visible-Light Catalysis and Adsorption. *Ind. Eng. Chem. Res.* **2016**, *55* (46), 12060–12067. https://doi.org/10.1021/acs.iecr.6b02178.

(6) Smith, K.; Liu, S. Energy for Conventional Water Supply and Wastewater Treatment in Urban China: A Review. *Glob. Challenges* **2017**, *1* (5), 1600016. https://doi.org/10.1002/gch2.201600016.

(7) Dichiara, A. B.; Weinstein, S. J.; Rogers, R. E. On the Choice of Batch or Fixed Bed Adsorption Processes for Wastewater Treatment. *Ind. Eng. Chem. Res.* **2015**, *54* (34), 8579–8586. https://doi.org/10.1021/acs.iecr.5b02350.

(8) Blanchard, G.; Maunaye, M.; Martin, G. Removal of Heavy Metals from Waters by Means of Natural Zeolites. *Water Res.* **1984**, *18* (12), 1501–1507. https://doi.org/10.1016/0043-1354(84)90124-6.

(9) Ho, Y. S.; McKay, G. Pseudo-Second Order Model for Sorption Processes. *Process Biochem.* **1999**, *34* (5), 451–465. https://doi.org/10.1016/S0032-9592(98)00112-5.

(10) Simonin, J. P. On the Comparison of Pseudo-First Order and Pseudo-Second Order Rate Laws in the Modeling of Adsorption Kinetics. *Chem. Eng. J.* **2016**, *300*, 254–263. https://doi.org/10.1016/j.cej.2016.04.079.

(11) Ho, Y. S.; Mckay, G. The Kinetics of Sorption of Divalent Metal Ions onto Sphagnum Moss Peat. *Water Res.* **2000**, *34* (3), 735–742.

(12) Ho, Y. Review of Second-Order Models for Adsorption Systems. *J. Hazard. Mater.* **2006**, *136* (April 2005), 681–689. https://doi.org/10.1016/j.jhazmat.2005.12.043.

(13) Plazinski, W.; Dziuba, J.; Rudzinski, W. Modeling of Sorption Kinetics: The Pseudo-Second Order Equation and the Sorbate Intraparticle Diffusivity. *Adsorption* **2013**, *19* (5), 1055–1064. https://doi.org/10.1007/s10450-013-9529-0.

(14) Xiao, Y.; Azaiez, J.; Hill, J. M. Erroneous Application of Pseudo-Second-Order Adsorption Kinetics Model: Ignored Assumptions and Spurious Correlations. *Ind. Eng. Chem. Res.* **2018**, *57* (7), 2705–2709. https://doi.org/10.1021/acs.iecr.7b04724.

(15) Canzano, S.; Iovino, P.; Leone, V.; Salvestrini, S.; Capasso, S. Use and Misuse of Sorption Kinetic Data: A Common Mistake That Should Be Avoided. *Adsorpt. Sci. Technol.* **2012**, *30* (3), 217–225. https://doi.org/10.1260/0263-6174.30.3.217.

(16) Qiu, H.; Lv, L.; Pan, B. C.; Zhang, Q. J.; Zhang, W. M.; Zhang, Q. X. Critical Review in Adsorption Kinetic Models. *J. Zhejiang Univ. Sci. A* **2009**, *10* (5), 716–724. https://doi.org/10.1631/jzus.A0820524.

(17) Ollis, D. F. Kinetics of Photocatalyzed Reactions: Five Lessons Learned. *Front. Chem.* **2018**, *6* (378), 1–7. https://doi.org/10.3389/fchem.2018.00378.

(18) Lützenkirchen, J.; Behra, P. On the Surface Precipitation Model for Cation Sorption at the (Hydr)Oxide Water Interface. *Aquat. Geochemistry* **1995**, *1* (4), 375–397. https://doi.org/10.1007/BF00702740.

(19) Bullen, J. C.; Saleesongsom, S. Adsorption Kinetics Data Sets, Compiled from the Literature. As Used in the Research Article "A Revised Pseudo-Second Order Kinetic Model for Adsorption, Sensitive to Changes in Adsorbate and Adsorbent Concentrations." *Zenodo*. January 15, 2021. https://doi.org/10.5281/ZENODO.4443102.

(20) Atkins, P.; Paula, J. De. *Atkins' Physical Chemistry*, 9th ed.; Oxford University Press, 2009. https://doi.org/10.1021/ed056pA260.1.

(21) Hu, W.; Xie, J.; Chau, H. W.; Si, B. C. Evaluation of Parameter Uncertainties in Nonlinear Regression Using Microsoft Excel Spreadsheet. *Environ. Syst. Res.* **2015**, *4* (1). https://doi.org/10.1186/s40068-015-0031-4.

(22) Kirby, M. E.; Bullen, J. C.; Hanif, M. D.; Heiba, H. F.; Liu, F.; Northover, G. H. R.; Resongles, E.; Weiss, D. J. Determining the Effect of PH on Iron Oxidation Kinetics in Aquatic Environments: Exploring a Fundamental Chemical Reaction to Grasp the Significant Ecosystem Implications of Iron Bioavailability. *J. Chem. Educ.* **2019**. https://doi.org/10.1021/acs.jchemed.8b01036.

(23) Yang, H.; Yu, H.; Fang, J.; Sun, J.; Xia, J.; Xie, W.; Wei, S.; Cui, Q.; Sun, C.; Wu, T. Mesoporous Layered Graphene Oxide/Fe3O4/C3N3S3 Polymer Hybrids for Rapid Removal of Pb2+ and Cd2+ from Water. *ACS Omega* **2019**, *4* (22), 19683–19692. https://doi.org/10.1021/acsomega.9b02347.

(24) Yang, X. Y.; Al-Duri, B. Application of Branched Pore Diffusion Model in the Adsorption of Reactive Dyes on Activated Carbon. *Chem. Eng. J.* **2001**, *83* (1), 15–23. https://doi.org/10.1016/S1385-8947(00)00233-3.

(25) Liu, Y.; Shen, L. From Langmuir Kinetics to First- and Second-Order Rate Equations for Adsorption. *Langmuir* **2008**, *24* (20), 11625–11630. https://doi.org/10.1021/la801839b.

(26) Zhu, Q.; Moggridge, G. D.; D'Agostino, C. Adsorption of Pyridine from Aqueous Solutions by Polymeric Adsorbents MN 200 and MN 500. Part 2: Kinetics and Diffusion Analysis. *Chem. Eng. J.* **2016**, *306*, 1223–1233. https://doi.org/10.1016/j.cej.2016.07.087.

(27) Yang, K.; Li, Y.; Zheng, H.; Luan, X.; Li, H.; Wang, Y.; Du, Q.; Sui, K.; Li, H.; Xia, Y. Adsorption of Congo Red with Hydrothermal Treated Shiitake Mushroom. *Mater. Res. Express* **2019**, *7* (1). https://doi.org/10.1088/2053-1591/ab5ff3.

(28) Yang, H.; Wang, Y.; Bender, J.; Xu, S. Removal of Arsenate and Chromate by Lanthanum-Modified Granular Ceramic Material: The Critical Role of Coating Temperature. *Sci. Rep.* **2019**, *9* (1), 1–12. https://doi.org/10.1038/s41598-019-44165-8.

(29) Mohamed, S. F.; Al-Bakri, I. M.; El Sayed, O. H. Biosorption of Lead (II) by Pre-Treated Biomass of Marine Brown Algae Sargassum Latifolium and Sargassum Asperifolium. *Biosci. Biotechnol. Res. Asia* **2007**, *4* (2), 341–350.

(30) Drenkova-tuhtan, A.; Mandel, K.; Meyer, C.; Schneider, M. Removal and Recovery of Phosphate from Wastewater with Reusable Magnetically Separable Particles. *IWA Spec. Conf. Nutr. Remov. Recover. Mov. Innov. into Pract.* **2015**, No. May. https://doi.org/10.13140/RG.2.1.1260.8721.

(31) Liu, J.; Wu, X.; Hu, Y.; Dai, C.; Peng, Q.; Liang, D. Effects of Cu(II) on the Adsorption Behaviors of Cr(III) and Cr(VI) onto Kaolin. *J. Chem.* **2016**, *2016* (Vi). https://doi.org/10.1155/2016/3069754.

(32) Örnek, A.; Özacar, M.; Şengil, I. A. Adsorption of Lead onto Formaldehyde or Sulphuric Acid Treated Acorn Waste: Equilibrium and Kinetic Studies. *Biochem. Eng. J.* **2007**, *37* (2), 192–200. https://doi.org/10.1016/j.bej.2007.04.011.

(33) Zhan, W.; Xu, C.; Qian, G.; Huang, G.; Tang, X.; Lin, B. Adsorption of Cu(Ii), Zn(Ii), and Pb(Ii) from Aqueous Single and Binary Metal Solutions by Regenerated Cellulose and Sodium Alginate Chemically Modified with Polyethyleneimine. *RSC Adv.* **2018**, *8* (33), 18723–18733.

https://doi.org/10.1039/c8ra02055h.

(34) Ai, T.; Jiang, X.; Liu, Q.; Lv, L.; Dai, S. Single-Component and Competitive Adsorption of Tetracycline and Zn(Ii) on an NH4Cl-Induced Magnetic Ultra-Fine Buckwheat Peel Powder Biochar from Water: Studies on the Kinetics, Isotherms, and Mechanism. *RSC Adv.* **2020**, *10* (35), 20427–20437. https://doi.org/10.1039/d0ra02346a.

(35) Nadiye-tabbiruka, M. S.; Sejie, F. P. Preparation of Coal-Kaolinite Nano Composites and Investigation of Their Use to Remove Methyl Orange from Water. **2019**, *9* (2), 37–43. https://doi.org/10.5923/j.nn.20190902.01.

(36) Largitte, L.; Pasquier, R. A Review of the Kinetics Adsorption Models and Their Application to the Adsorption of Lead by an Activated Carbon. *Chem. Eng. Res. Des.* **2016**, *109*, 495–504. https://doi.org/10.1016/j.cherd.2016.02.006.

(37) Azizian, S. Kinetic Models of Sorption: A Theoretical Analysis. *J. Colloid Interface Sci.* **2004**, *276* (1), 47–52. https://doi.org/10.1016/j.jcis.2004.03.048.

(38) Marczewski, A. W. Analysis of Kinetic Langmuir Model. Part I: Integrated Kinetic Langmuir Equation (IKL): A New Complete Analytical Solution of the Langmuir Rate Equation. *Langmuir* **2010**, *26* (19), 15229–15238. https://doi.org/10.1021/la1010049.

(39) Bullen, J. C.; Lapinee, C.; Salaün, P.; Vilar, R.; Weiss, D. J. On the Application of Photocatalyst-Sorbent Composite Materials for Arsenic(III) Remediation: Insights from Kinetic Adsorption Modelling. *J. Environ. Chem. Eng.* **2020**, *8* (5). https://doi.org/10.1016/j.jece.2020.104033.

(40) Manna, B. R.; Dey, S.; Debnath, S.; Ghosh, U. C. Removal of Arsenic from Groundwater Using Crystalline Hydrous Ferric Oxide (CHFO). *Water Qual. Res. J. Canada* **2003**, *38* (1), 193–210. https://doi.org/10.2166/wqrj.2003.013.

(41) Singh, D. B.; Prasad, G.; Rupainwar, D. C. Adsorption Technique for the Treatment of As(V)-Rich Effluents. *Colloids Surfaces A Physicochem. Eng. Asp.* **1996**, *111* (1–2), 49–56. https://doi.org/10.1016/0927-7757(95)03468-4.

(42) Mezenner, N. Y.; Bensmaili, A. Kinetics and Thermodynamic Study of Phosphate Adsorption on Iron Hydroxide-Eggshell Waste. *Chem. Eng. J.* **2009**, *147* (2–3), 87–96. https://doi.org/10.1016/j.cej.2008.06.024.

(43) Debnath, A.; Bera, A.; Chattopadhyay, K. K.; Saha, B. Facile Additive-Free Synthesis of Hematite Nanoparticles for Enhanced Adsorption of Hexavalent Chromium from Aqueous Media: Kinetic, Isotherm, and Thermodynamic Study. *Inorg. Nano-Metal Chem.* **2017**, *47* (12), 1605–1613. https://doi.org/10.1080/24701556.2017.1357581.

(44) Lazaridis, N. K.; Pandi, T. A.; Matis, K. A. Chromium(VI) Removal from Aqueous Solutions by Mg-Al-CO3 Hydrotalcite: Sorption-Desorption Kinetic and Equilibrium Studies. *Ind. Eng. Chem. Res.* **2004**, *43* (9), 2209–2215. https://doi.org/10.1021/ie030735n.

(45) Shipley, H. J.; Engates, K. E.; Grover, V. A. Removal of Pb(II), Cd(II), Cu(II), and Zn(II) by Hematite Nanoparticles: Effect of Sorbent Concentration, PH, Temperature, and Exhaustion. *Environ. Sci. Pollut. Res.* **2013**, *20* (3), 1727–1736. https://doi.org/10.1007/s11356-012-0984-z.

(46) Ayawei, N.; Ebelegi, A. N.; Wankasi, D. Modelling and Interpretation of Adsorption Isotherms. *J. Chem.* **2017**, *2017*. https://doi.org/10.1155/2017/3039817.

(47) Huang, Y.; Farooq, M. U.; Lai, S.; Feng, X.; Sampranpiboon, P.; Wang, X.; Huang, W. Model Fitting of Sorption Kinetics Data: Misapplications Overlooked and Their Rectifications. *AIChE J.* **2018**, *64* (5), 1793–1805. https://doi.org/10.1002/aic.16051.

(48) Cooney, D. O.; Adesanya, B. A.; Hines, A. L. Effect of Particle Size Distribution on Adsorption Kinetics in Stirred Batch Systems. *Chem. Eng. Sci.* **1983**, *38* (9), 1535–1541. https://doi.org/10.1007/978-1-4419-8074-8_10.

(49) Simonin, J.; Boute, J. Intraparticle Diffusion-Adsorption Model to Describe Liquid/Solid Adsorption Kinetics. *Rev. Mex. Ing. Quim.* **2016**, *15* (1), 161–173.